The Egyptian Journal of Remote Sensing and Space Sciences 24 (2021) 319–328

Contents lists available at ScienceDirect

The Egyptian Journal of Remote Sensing and Space Sciences

journal homepage: www.sciencedirect.com

Evaluation of the MOD16A2 evapotranspiration product in an agricultural area of Argentina, the Pampas region

María Florencia Degano [a,b,*], Raúl Eduardo Rivas [a,b], Facundo Carmona [a,c], Raquel Niclòs [d], Juan Manuel Sánchez [e]

[a] Instituto de Hidrología de Llanuras Dr. Eduardo J. Usunoff, Universidad Nacional del Centro de la Provincia de Buenos Aires, Pinto 399, Tandil 7000, Argentina
[b] Comisión de Investigaciones Científicas (CIC), Buenos Aires, Argentina
[c] Consejo Nacional de Investigaciones Científicas y Técnicas (CONICET), Buenos Aires, Argentina
[d] Departamento de Física de la Tierra y Termodinámica, Universidad de Valencia, Burjassot 46100, Spain
[e] Instituto de Desarrollo Regional, Departamento de Física Aplicada, Universidad de Castilla-La Mancha, Albacete 02071, Spain

ARTICLE INFO

Article history:
Received 2 October 2019
Revised 18 August 2020
Accepted 26 August 2020
Available online 8 September 2020

Keywords:
Actual evapotranspiration
Ground measurements
MOD16A2 version 6
Potential evapotranspiration
Remote sensing

ABSTRACT

The Pampas Region is a big plain of approximately 520,000 km^2 in Argentina. It is essential to estimate evapotranspiration (ET) in this region since the primary productivity is directly linked to water availability. Information provided by satellite missions allows monitoring the spatial and temporal variability of ET. In the current study, we evaluated the version 006 of MOD16A2 product (MOD16A2.006) of Potential Evapotranspiration (ETp) and Actual Evapotranspiration (ETa) in Argentinian Pampas Region (APR). MOD16A2.006 product was compared with Crop Evapotranspiration (ETc), calculated with local measurements from the *Oficina de Riesgo Agropecuario* (ORA), and Crop Coefficient (Kc) data (function of Normalized Difference Vegetation Index (NDVI)) in seven stations in the APR from 2009 to 2018. We evaluated ETa at two temporal scales: accumulated values (mm) per growth stages (soybean crop), and 8-day accumulated values (mm8d^{-1}). The results showed a systematic overestimation around 65% for $ETp_{(MOD16A2.006)}$ (found and eliminated by means of a linear function) and underestimation (in most stations) for $ETa_{(MOD16A2.006)}$ in accumulated values per growth stages. Respect to mm8d^{-1}, no systematic error was observed, but the relationship $ETa_{(ORA)} - ETa_{(MOD16A2.006)}$ for soybean crop behaves similarly throughout APR.

1. Introduction

In 2015, the United Nations Development Program (UNDP), promoted the adoption by member countries of 17 Sustainable Development Goals (SDGs), considered fundamental pillars to combat inequality, poverty, protect the planet and ensure that all people in the world enjoy a better quality of life. According to SDGs, and particularly goal 2″Zero Hunger"; 6"Clean Water and Sanitation" and 13"Climate Action", a detailed study of the water flows involved in the planet's hydrological cycle is essential (https://sustainabledevelopment.un.org).

Since planet Earth is a heterogeneous and variable system, it is important to know and study climate variability, establish the extremes within the hydrological cycle and determine how its different components vary and interact. Within the different meteorological processes that continuously occur in the atmosphere, the most important parameter to quantify for application in the fields of climatology, meteorology, hydrology and agronomy are those related to water flows (precipitation and ET), in which the atmosphere interacts with surface.

The Pampas Region is a big plain of approximately 520,000 km^2 in Argentina (Pereyra, 2003). ET is the hydrological variable of greatest relevance in this area because it accounts for a large part (greater than80%) of the precipitation incomes. This hydrological term becomes even more relevant in the APR since the primary productivity of the region is agriculture and depends strongly on the water available to evapotranspiration process.

Peer review under responsibility of National Authority for Remote Sensing and Space Sciences.

* Corresponding author at: Instituto de Hidrología de Llanuras Dr. Eduardo J. Usunoff, Universidad Nacional del Centro de la Provincia de Buenos Aires, Pinto 399, Tandil 7000, Argentina.

E-mail addresses: mfdegano@ihlla.org.ar (M.F. Degano), rrivas@rec.unicen.edu.ar (R.E. Rivas), facundo.carmona@rec.unicen.edu.ar (F. Carmona), raquel.niclos@uv.es (R. Niclòs), juanmanuel.sanchez@uclm.es (J.M. Sánchez).

https://doi.org/10.1016/j.ejrs.2020.08.004
1110-9823/

Currently, there are different methods to estimate the ET. At point scale: porometers, flow meters of sage in the plant and lysimeters; on a pilot scale, water balances, Bowen relation, Eddy Covariance (EC) systems, centillometers, among others; and at the regional level, incorporating mainly satellite data (Carmona et al., 2018).

Due to advances in remote sensing technology and methods, there are numerous models to obtain ET products with satellite data capturing the space–time variability of this parameter. Some methods based on satellite data are: energy balance methods; methods based on the relationship between vegetation index and surface temperature; methods based on the Penman-Monteith (PM) equation; methods based on the Priestley-Taylor equation; empiric methods and water balance methods (Carmona, et al., 2018; Zhang et al., 2016).

As summarized in Chang et al. (2018), Cleugh et al. (2007) developed an ETa/ETp satellite product based on the PM equation using data from the Moderate Resolution Imaging Spectroradiometer (MODIS) and reanalysis meteorological data (Cleugh et al., 2007). Mu et al. (2007) modified this product and produced the first global MODIS ET dataset with a spatial resolution of 1 km and temporal resolution of 8-day, monthly and annual. Mu et al. (2011) further improved the MODIS ET algorithm to derive a more accurate MODIS global ET product (Version005 MOD16A2.005). Finally, in updated version006 ($ET_{(MOD16A2.006)}$ product), the spatial resolution was improved to 500 m. The nighttime actual vapor pressure, nighttime temperature, outgoing and incoming longwave radiation are obtained from Modern-Era Retrospective analysis for Research and Applications (MERRA) data directly (Running et al., 2017).

Some authors (Table 1) evaluated the performance of MOD16A2.005/006 products around the world, based on the comparison with ground ETa/ETp measurements (e.g., EC). The results indicated that the reliability of both MOD16A2 product were not consistent enough to be used as an indicator of ET in the variety of environmental conditions studied.

In particular, acceptable results were found by Aguilar et al. (2018), to consider the applicability of $ETa_{(MOD16A2.006)}$ products in areas with close shrubs, at a regional, state, and basin scale, in arid and semiarid zones, despite the error, bias, and medium concordance indices found between EC and MOD16A2.006. However, not enough evidence was obtained by these authors to recommend the use of MOD16 in crops. Also, in most cases, MOD16A2.006 underestimated ETa values.

Chang et al. (2018) showed that the MOD16A2.006 algorithm tended to underestimate ET at high values and overestimate it at low values, which induced substantial uncertainties in Tibetan Plateau, China. In Peschechera et al. (2018), the authors made a comparison between the $ET_{(MOD16A2.006)}$ product and the ET calculated with an analytical approach in a large cultivated area of the irrigation district "Sinistra Ofanto" in Apulian Tavoliere (Italy), throughout the year 2016. The statistical analysis determined an overestimation of $ETp_{(MOD16A2.006)}$ of around 8.63 $mm8d^{-1}$, with the only exception for the spring season.

In relation to ETp, Degano et al. (2018b) evaluated in APR the relationship between MOD16A2.005 product (Mu et al., 2013) and reference evapotranspiration (ET_0) from ORA. A systematic overestimation for MOD16A2.005 was observed. In this sense, the main objective of this paper is determining the performance of the $ETp_{(MOD16A2.006)}$ product (Running et al., 2017) for the agricultural area of Argentina, and specifically evaluating the product by comparison against ETc ORA data.

Since agriculture is the main economical source in APR, the determination of ETa becomes crucial. In recent decades, world soybean production grew by 44%. Argentina became the third producer country after United States and Brazil (Reboratti, 2010). In this context, in APR, soybean came to occupy around 60% of the cultivated area. In order to evaluate the $ETa_{(MOD16A2.006)}$, it was compared with $ETa_{(ORA)}$ data on soybean cultivation.

Since the MOD16A2.006 product is widely used in the APR for different purposes (e.g., calculation of the water footprint), it needs to be evaluated. Therefore, the main objective of this paper is to determine the performance of ETp-ETa variables provided by the MOD16A2.006 product in this region. In both cases, local data from the ORA are used as reference for analysing the relationships between $ETc_{(ORA)}$ and $ETp_{(MOD16A2.006)}$, and between $ETa_{(ORA)}$ and $ETa_{(MOD16A2.006)}$. Thus, the specific objectives of this study are: (a) to evaluate the product with data acquired at seven stations in the APR; (b) to determine the variation of ETp-ETa according to the variability of water availability in different years (2009–2018); (c) analyse ETa in different soybean growth stages and (d) to determine the errors of the product for each zone.

2. study area

APR is an extensive plain located in the central-eastern area of Argentina that includes five agricultural provinces: South of Entre Ríos, South-East of Córdoba, South of Santa Fe, East of La Pampa and the most area of Buenos Aires province. APR is divided in different ecoregions, in this paper we use data from seven stations distributed in the different ecoregions (Fig. 1-Table 2). Table 2 includes APR's edaphoclimatic characteristics considered in the soil water balance.

Also, the Köppen classification (Kottek et al., 2006) subdivides the APR according to climatic characteristics, considering, mainly, the annual and monthly average temperature and precipitation values. In this context, the stations 1, 2, 3, 4 y 6 (South of Santa Fe, South of Entre Ríos and East of Buenos Aires) belong to Subhumid-Humid Pampas and the stations 5 and 7 (East of La Pampa and West of Buenos Aires) belong to Semiarid Pampas.

3. Methodology

3.1. Satellite data processing

The MOD16A2.006 data are provided by Earth Data-National Aeronautics and Space Administration (NASA). The algorithm is based on the PM equation. Inputs come from the reanalysis global daily meteorological dataset MERRA and from MODIS data: land $cover_{(MOD12Q1)}$ product; Leaf Area Index/Fraction of Photosynthetically Active Radiation ($LAI/FPAR_{(MOD15)}$ product) and $Albedo_{(MCD43A2/A3)}$ product. This product is based on the algorithm first proposed by Mu et al. (2011), however, since then, some updates have been implemented in the operational code to fix some issues. These updates are detailed in Running et al. (2017).

The methodological flowchart is shown in Figs. 4 and 5. MOD16A2.006 product provides data with a spatial resolution of 500 m and corresponding to 8-days accumulated values. To process this product, first, we downloaded the product (http://files.ntsg.umt.edu/data/NTSG_Products/MOD16/), then, we extracted bands ETp-ETa correspond, after that, we re-projected the product with "MODIS conversion toolkit" in Environment for Visualizing Images (ENVI). Then, we determined a kernel of 3x3 pixels, and ETp-ETa data were obtained. Finally, we filtered data (we excluded values that were outside the 95% confidence interval). To clarify, the images are available in Hierarchical Data Format-Earth Observing System (HDF-EOS) format, covering about 1200x1200-km^2. Even though Running et al. (2017) suggested that users may ignore QC data layer because cloud-contaminated LAI/FPAR gaps have been temporally filled before calculating ET, for the improved and reprocessed MOD16A2, it was necessary to perform a data

Table 1
Overview of studies evaluating and comparing MOD16A2.005/006 data with ground measurements. Unit unified to $mm8d^{-1}$ • Reference method: EC *Reference method: PM equation.

Reference	Site	Punctual Data	Period	ET	R^2	RMSE [$mm8d^{-1}$]	MOD16 version
Ruhoff et al. (2013)	Rio Grande basin, Brazil	Sugar-cane plantation•	2001	ETa	0.78	6.2	005
		Natural Savannah•			0.81	3.7	
Nadzri and Hashim (2014)	South East Asia	Peninsular Malasya	2000–2009	ETp	0.33	9.9	005
Ramoelo et al. (2014)	South Africa	African Savannah, Skukuza•	2000	ETa	0.26	5.2	005
			2001		0.35	3.6	
			2003		0.58	3.4	
			2004		0.54	8.0	
			2005		0.81	2.0	
			2007		0.85	6.0	
			2008		0.36	7.4	
			2009		0.78	7.4	
			2010		0.74	4.3	
		African Savannah, Malopeni•	2009		0.23	3.0	
Hu et al. (2015)	Europe	Oensingen crop(winter wheat)•	2009–2011	ETa	0.90	5.8	005
		Klingenberg(winter barley)•			0.91	3.8	
		Monte Bondone(meadow)•			0.92	4.7	
		Cabauw(meadow)•			0.95	4.5	
		Amoladeras(dwarf shrub)•			0.29	2.6	
		Llano de los Juanes(matorral shrub)•			0.42	3.2	
		Las Majadas del Tietar(holm oak open woodland)•			0.78	9.4	
		Brasschaat(Scots pine, English oak)•			0.94	6.9	
		Collelongo(European beech)•			0.70	10.1	
		Roccarespampani(Turkey oak)•			0.88	12.6	
		Puechabon(holm oak)•			0.89	3.3	
		Bily Kriz forest(Norway spruce)•			0.85	7.1	
		Tharandt(Norway spruce)•			0.93	6.3	
		San Rossore(maritime pine)•			0.45	8.6	
		Fyodorovskoye(wet spruce)•			0.98	2.7	
Autovino et al. (2016)	South Western Sicily, Italy	Castelvetrano•	2011–2014	ETa	0.23	6.6	005
Aguilar et al. (2018)	North Mexico	Valle de Yaqui$_{1,2}$•Crop-Closed Shrub	2008	ETa	0.43	9.8	006
		Rayón•	2008–2010		0.86	6.2	
		El Mogor•, Open Shrub			0.44	3.2	
		La Paz•, Open Shrub	2004–2006				
Chang et al. (2018)	Tibetan Plateau, China	Suli•	2010–2011-2013–2014	ETp	0.11	13.8	006
		Nagqu•			0.38	14.9	
		Tanggula•			0.11	18.5	
		Hulugou•			0.95	8.7	
Peschechera et al. (2018)	Italy	Sinistra Ofanto(vineyards, olive trees, orchards and cereals)*	2016	ETa	0.53	7.1	006
				ETp	0.95	8.6	
Degano et al. (2018b)	Argentina	Argentina Pampas Region*	2012–2014	ETp	0.86	19.2	005

filtering, and those data outside the valid range were discarded from the analysis.

3.2. Ground data

3.2.1. ETc data

According to methodology flowchart in Fig. 4, ORA dataset provide ET_0, this is calculated with the PM equation (1) (Monteith and Unsworth, 1990) with information provided by the *Servicio Meteorológico Nacional* (SMN) of Argentina:

$$ET_0 = \frac{0.408\Delta(RN - G) + \frac{900}{T+273}u_2(VPD)}{\Delta + \gamma(1 + 0.34u_2)} \quad (1)$$

where RN is net radiation at the crop surface [$MJm^{-2}d^{-1}$], G is soil heat flux density [$MJm^{-2}d^{-1}$], T is mean daily air temperature at 2-m height [°C], u_2 is wind speed at 2-m height [ms^{-1}], 0.408 is a conversion factor to mmd^{-1}, 900 is coefficient for the reference crop [$kJ^{-1}KgKd^{-1}$], 273 is conversion factor to express the temperature in K and 0.34 is a coefficient resulting from assuming a crop resistance of 70 sm^{-1} and an aerodynamic drag of 208/u_2 for the reference crop [sm^{-1}]. ET_0 [mmd^{-1}] is provided at daily scale, to compare with MOD16A2.006 product it is necessary to convert the temporal resolution to $8d^{-1}$. It should be noted that the SMN dataset are measurements acquired from the stations. The data completion procedure was not used.

According to Allen et al. (1998), the differences in leaf anatomy, stomata characteristics, aerodynamic properties and even albedo cause differences between ETc and ET_0 under the same climatic conditions. Due to variations in the crop characteristics throughout its growing season, Kc for a given crop changes from sowing till harvest. So, it was necessary to calculate ETc for the evaluation (Eq. (2)).

$$ETc = ET_0 x Kc_{NDVI} \quad (2)$$

where Kc_{NDVI} is the crop coefficient calculated with the linear equation obtained following the methodology of Kamble et al. (2013). Fig. 2 shows the relationship between the soybean Kcs and NDVIs for rainfed agriculture sites. There was a strong correlation between Kc and NDVI for the five stations in the APR shown in the figure. The regression equation is shown for the data of the five stations altogether.

According to Fig. 2, the Kc_{NDVI} used in Eq. (2) is determined by:

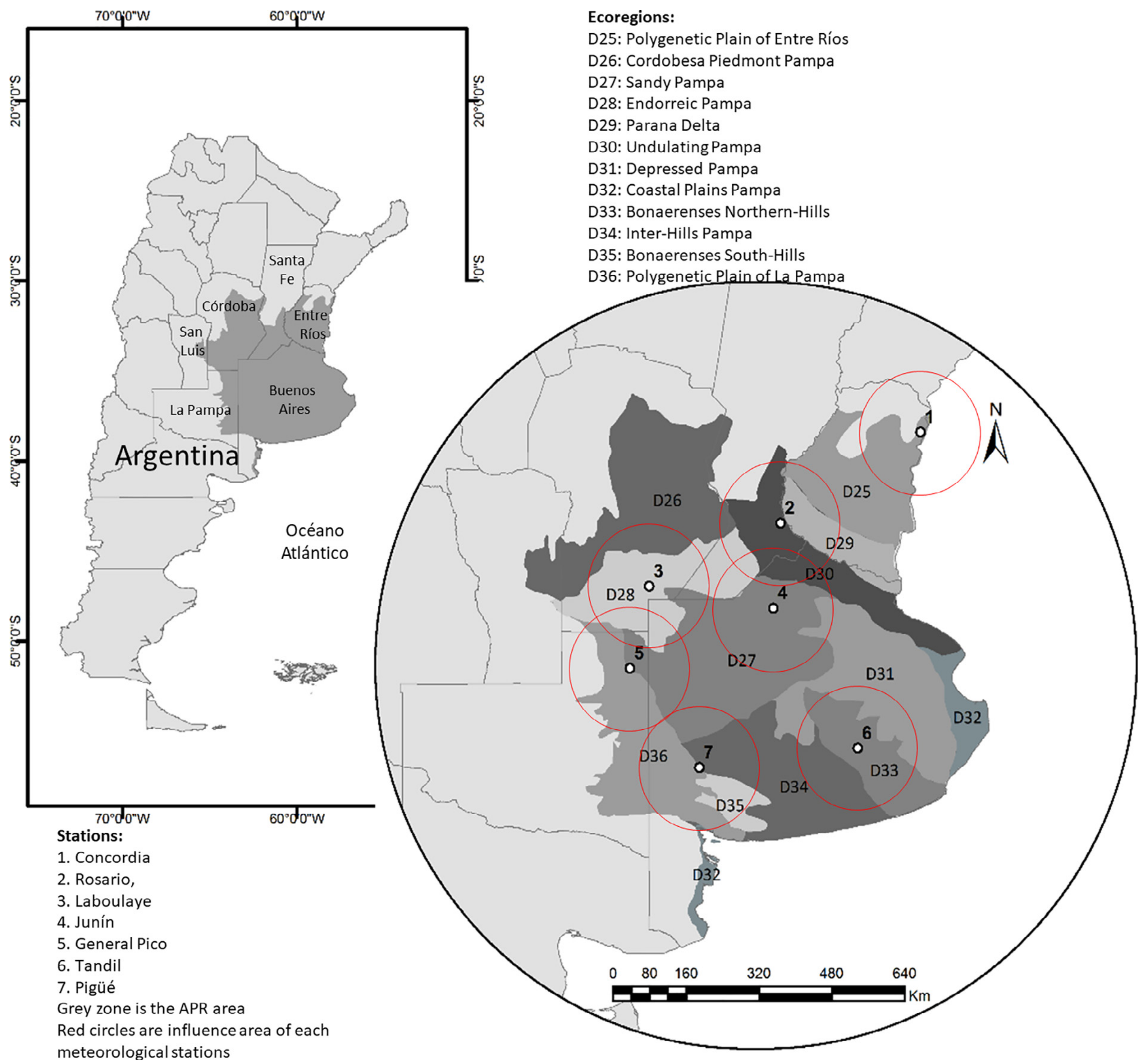

Fig. 1. APR and spatial distribution of influence area of meteorological stations (Modified from Carmona et al., 2018).

$$Kc_{NDVI} = 1.41xNDVI - 0,17 \quad (3)$$

The MOD13A1.006 NDVI product is 500 m spatial resolution. The algorithm chooses the best available pixel value from all the acquisitions from the 16-days period. The criteria used is minimum cloud coverage, low view angle, and the highest NDVI value (Didan et al., 2015). We used a 16-days NDVI product because this temporal resolution is quite representative of the region variability, since this variable does not change as abruptly as the temperature, for example.

According to Fig. 4, respect to ground measurements, we obtained ETc (calculated with ET_{0ORA}-and Kc_{NDVI} data) and converted data from mmd^{-1} to $mm8d^{-1}$. For validation we compared $ETp_{MOD16A2.006}$ to ETc $_{ORA}$ with different statistical estimates (section 3.2.3). With respect to spatiality, we compared kernels of 3x3pixels (1.5-km × 1.5-km) MOD16A2.006 product with ORA data of SMN meteorological stations that covers a radius of 127 km in plains zones as APR (Fig. 1, WMO, 1994).

3.2.2. Ground ETa

ETa is calculated by ORA with soil water balance method. The method consists of assessing the incoming and outgoing water flux into the crop root zone over some time period (Fig. 3). I and P add water to the root zone. Part of I and P might be lost by surface RO and by DP that will eventually recharge the water table. Water might also be transported upward by CR from a shallow water table towards the root zone or even transferred horizontally by SFin or out SFout the root zone. However, in many situations, except under conditions with large slopes, SFin and SFout are minor and can be ignored. Soil evaporation and crop transpiration deplete water from the root zone. If all fluxes other than evapotranspiration (ET) can be assessed, the evapotranspiration can be deduced from the change in soil water content (ΔSW) over the time period (Eq.4) (Allen et al., 1998):

$$ETa = I + P - RO - DP + CR \pm \Delta SF \pm \Delta SW \quad (4)$$

$ETa_{(ORA)}$ [mmd^{-1}] data is provided at daily scale, it was necessary data conversion to $mm8d^{-1}$ and then, we rescaled in mm per growth stages for the 2009–2018 period (Fig. 5). It should be noted, that soybean is sown early November and harvested at the end of March. Also, we filtering data we excluding values that were outside the 95% confidence interval.

Table 2
Edaphoclimatic characteristics of the analysed ecoregions. (Pereyra, 2003; Kottek et al., 2006) M: Moisture T: Mean annual air temperature, P: Rainfall, RH: Relative Humidity.

ID/Station	Landscape	Weather				Soil M/T regime	Predominant soil type
		Type		Warm Temperate			
		T (°C)	P (mmy^{-1})	RH (%)	ETp (mmy^{-1})		
D25/1. Concordia	Fluvial processes predominance	19	1100	75	1100	Udic	Alfisols-Mollisols-Vertisols-Entisols
D26	Fluvial processes, boxed rivers, 300 m elevation difference	19	700–800	50	1100	Ustic-Thermic	Mollisols
D27/4.Junín	Wind processes predominance, presence of dunes	18	800	60	1000	Udic	Tipics Argiudolls
D28/3. Laboulaye	Wind and fluvial processes predominance	18	900	60	1050	Udic-Ustic	Hapludolls- Haplustolls
D29	Delta environment with wide flooded interdistrict plains	18	1100	75	1000	Aquic	Entisols-Mollisols
D30/2.Rosario	Softly wavy relief. Deposit of silty material and fluvial processes	18	1100	70	1100	Udic-Thermic	Tipics Argiudolls
D31	Fluvial, coastal and wind processes predominance	16	1100	70	950	Aquic	Mollisols-Alfisols
D32	Soft relief. Deposition and erosion marine littoral	16	1100	70	1000	Aquic	Mollisols-Entisols-Vertisols-Alfisols
D33/6.Tandil	To North, important fluvial processes	16	1100	70	1100	Udic-Thermic	Tipics Argiudolls-Hapludolls
D34/7.Pigüé	Fluvial and wind processes predominance	16	900	70	950	Udic-Thermic	Tipics-Aquics Argiudolls
D35	Saws with marked agreement of summits	14	900	70	900	Udic-Thermic	Mollisols-Entisols
D36/5. General Pico	Softly wavy relief. Valleys with medanosos cords and water bodies. Greater aridity to West	16	800	60	1050	Ustic-Aridic	Haplustolls

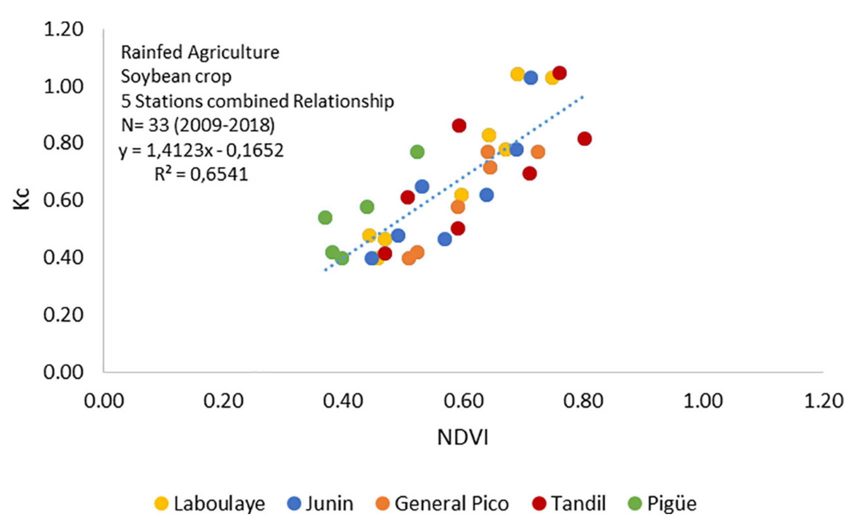

Fig. 2. Relationship between MOD13A1.006-NDVI and ORA measured soybean Kcs under rainfed crop condition.

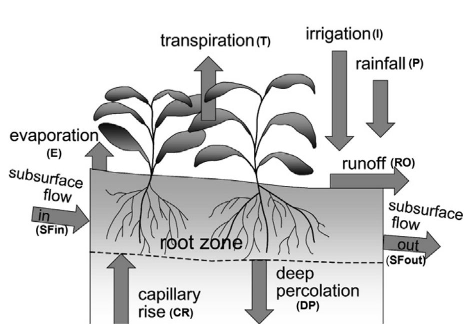

Fig. 3. Soil water balance method used by ORA.

3.3. Validation

3.3.1. Validation analysis

Following the scheme in Figs. 4 and 5, a statistical analysis was carried out after data processing and filtering. Classical statistics parameters were used: Root Mean Square Error (RMSE), Mean Absolute Error (MAE), Mean Absolute Percentual Error (MAPE), Determination Coefficient (R^2), slope (a) and intercept (b).

3.3.2. Errors correction

Following methodology of Degano et al. (2018a), the authors observed a systematic error in $ETp_{(MOD16A2.005)}$, we corrected systematic errors of the $ETp_{(MOD16A2.006)}$. To conduct this correction, we used 499 data pairs $ETp_{(MOD16A2.006)}$-$ETc_{(ORA)}$, which 50% was

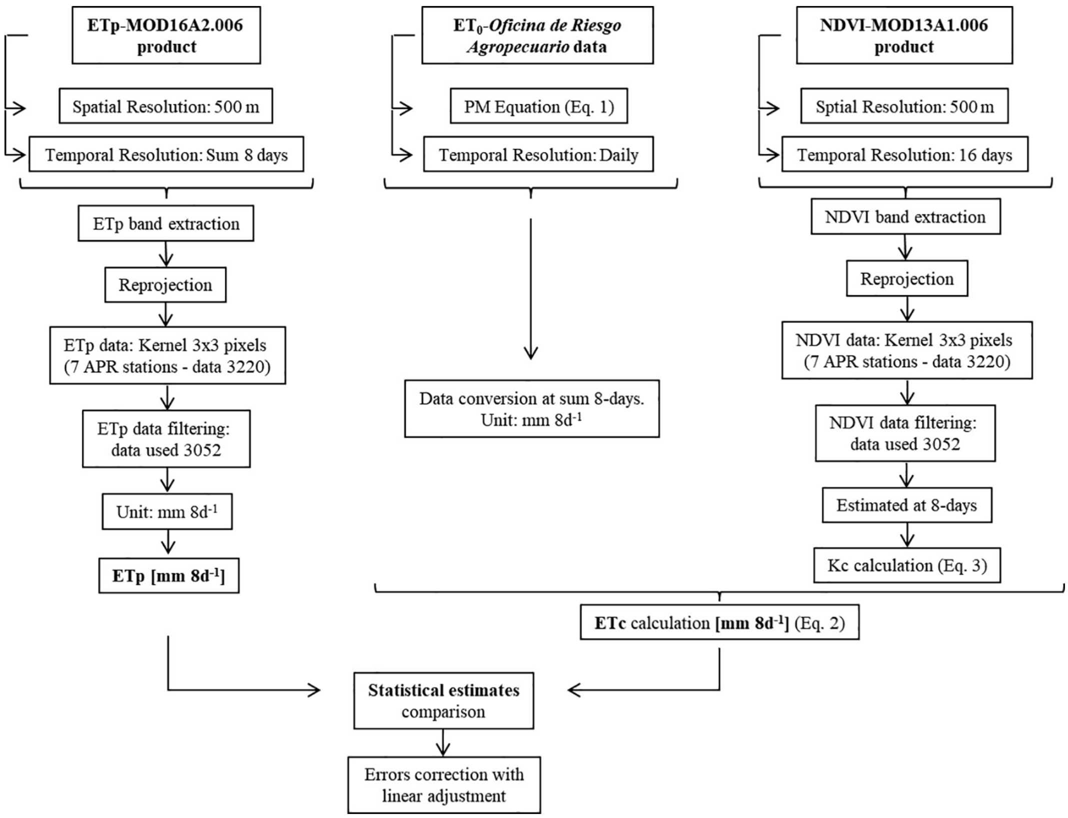

Fig. 4. Applied methodology flowchart for ETp-ETc.

used to obtain the linear adjustment equation (5) and the remaining 50% to calibrate.

$$MOD16A2.006_{Corrected} = 0.4ETp_{(MOD16A2.006)} - 0.2 \quad (5)$$

4. Results and discussion

4.1. Comparison between $ETp_{(MOD16A2.006)}$ product and $ETc_{(ORA)}$

In APR, Degano et al. (2018b) found that the $ETp_{(MOD16A2.005)}$ product overestimates more than 50%. The statistical analysis determined a RMSE of 2.4 mmd^{-1}. This error is might be partially due to the calculation of the incoming long wave radiation ($Rl_{\downarrow}$) which is calculated with an empirical model. This model in APR showed artificially large errors values, producing an overestimation of 1.1 mm d^{-1} in ETp. The rest of error is might be due to expected from remote sensing measurement system which is around 20% (1.3 mm d^{-1}) (Allen et al., 2011). In the improved version (MOD16A2.006), $Rl_{\downarrow}$ is not calculated with this empiric method, else is used on MERRA directly. We expect that MOD16A2.006 product would have a smaller error.

In this context, we used statistical metrics for comparison of the $ETp_{(MOD16A2.006)}$ product with $ETc_{(ORA)}$ data (Table 3). We observed a RMSE and MAE around 25 $mm8d^{-1}$ (3.2 mmd^{-1}), a is 1.8, b is 11.6 $mm8d^{-1}$ and $R^2 = 0.85$. When comparing $ETp_{(MOD16A2.006)}$ data with $ETc_{(ORA)}$ data, the results show an overestimation (Fig. 6), with a MAPE value around 65%. The errors are comparable to those obtained by several authors in different regions for MOD16A2.006 product (Table 1), e.g., in China, although a little greater in the case of Italy.

The systematic error indicates that MOD16A2.006 product is not suitable for estimating ETp directly in APR; hence it is necessary to correct this data product used a lineal adjustment equation (Eq. (5)-Fig. 6) (Degano et al., 2018a). After correction, the errors decrease significantly (Table 3), and product results improve considerably (Fig. 6). RMSE and MAE are reduced around 85%, the slope comes close to 1, and the intercept decreases to 4.4 $mm8d^{-1}$.

4.2. Comparison between $ETa_{(MOD16A2.006)}$ product and $ETa_{(ORA)}$

Soybean cultivation covers large areas in APR and this ensures a consistent assessment of the evapotranspiration process, since there are not border effects and the product evaluation has no bias. We evaluated ETa at two temporal scales: in mm per growth stages according to soybean growth stages, and in $mm8d^{-1}$.

Fig. 7 includes the results for accumulated values of $ETa_{(MOD16A2.006)}$ and $ETa_{(ORA)}$ data for three growth stages studied. When we compared ETa data in temporal resolution to $mm8d^{-1}$, a significant difference is observed in terms of ETa at 8-day temporal resolution between ORA data and MOD16A2.006 product data. The error is not systematic, but it varies depending on the station, years, and water availability (Fig. 8). In general, the behaviour of ground data shows an underestimation from early growth stages, towards the final, with some intermediate variations.

The performance of the MOD16A2.006 product depends on the zone. In Concordia (Subhumid-Humid), $ETa_{(MOD16A2.006)}$ product reproduces ground values at early growth stages, but towards final of growth stages differences are greater, being the satellite data greater than ground data. In Undulating Pampa (Rosario), the difference between both ETa is greater at early growth stages, decreasing towards the end of the growing season. A similar behaviour is shown in Laboulaye and Junín. In these zones, $ETa_{(ORA)}$ values are over $ETa_{(MOD16A2.006)}$ values. In general, the satellite product underestimate in semiarid zones too (General Pico and Pigüé). In Bonaerenses Northern Hills (Tandil), we observed a sig-

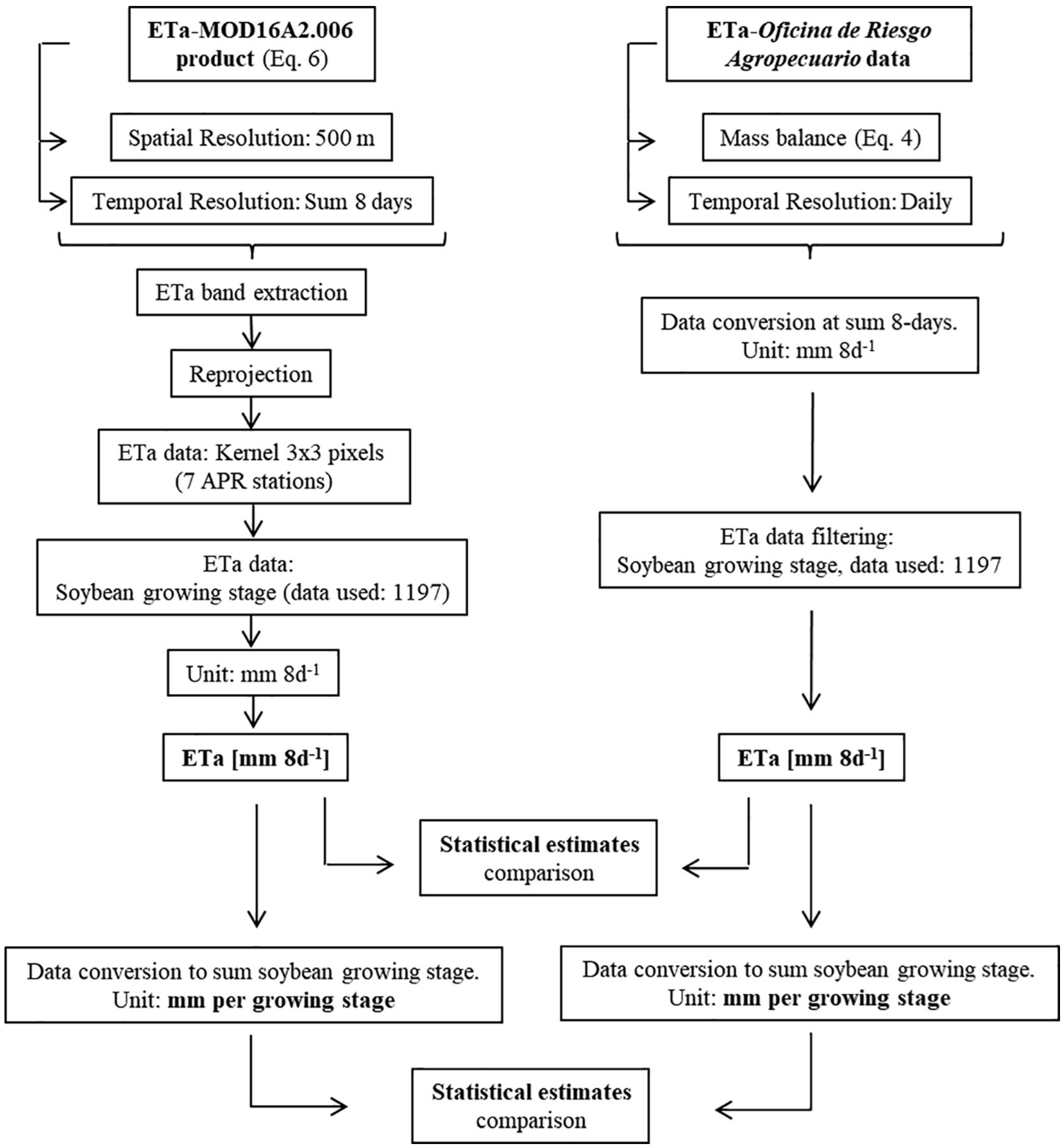

Fig. 5. Applied methodology flowchart for ETa.

Table 3
Statistical metrics for original and corrected MOD16A2.006 product.

Statistic [$mm8d^{-1}$]	Original data	Corrected data
RMSE	27.4	4.6
MAE	24.6	3.5
a [adimensional]	1.8	0.7
b	11.6	4.4
R^2	0.85	0.85

nificant deviation from MOD16A2.006 product, being greater than ORA data in most growth stages.

The amount of evapotranspirated water on the surface depends on the availability of water in each ORA station, on rainfall, and the stored water, which is a function of the type of soil. Analysing the growth stage levels in different stations (in the APR the precipitations are concentred between October to April, with dry winter), during the considered period, we observed growth stages with maximum precipitations (2009–2010) and minimum precipitations (2017–2018), for example.

It should be noted that in the analysed period, 2009–2018, the most important drought for the APR of the last 70 years was presented, with minimum rainfall concentrated in the critical months for soybean cultivation (January and February 2017–2018). The MOD16A2.006 product underestimates ETa for this period (Fig. 7- blue box, full line, right) with minimal accumulative differences in most stations. It was not the case for Concordia and Tandil stations, where satellite product overestimated significantly. It could be due to the site soils with high clay content. The clay has a low albedo (between 0.11 and 0.15), which can affect significantly the RNsoil value in the estimation of the $ETa_{(MOD16A2.006)}$ product, increasing this value. It is taken into account for the ETa calculation (Running et al., 2017). However, RNsoil is lower in soils with a higher percentage of sand or silt (albedo between 0.18 and 0.20).

For a wet year (red box, full line, left) a similar behavior is shown, with an underestimation observed for the $ETa_{(MOD16A2.006)}$ product in most stations, and with an overestimation in the Concordia and Tandil stations less significant than that for an extreme agronomic drought situation. In this growth stage, the effect of surface albedo is also observed, to a lesser extent (although the albedo is less in wet clay). However, the effect is less significant due to the

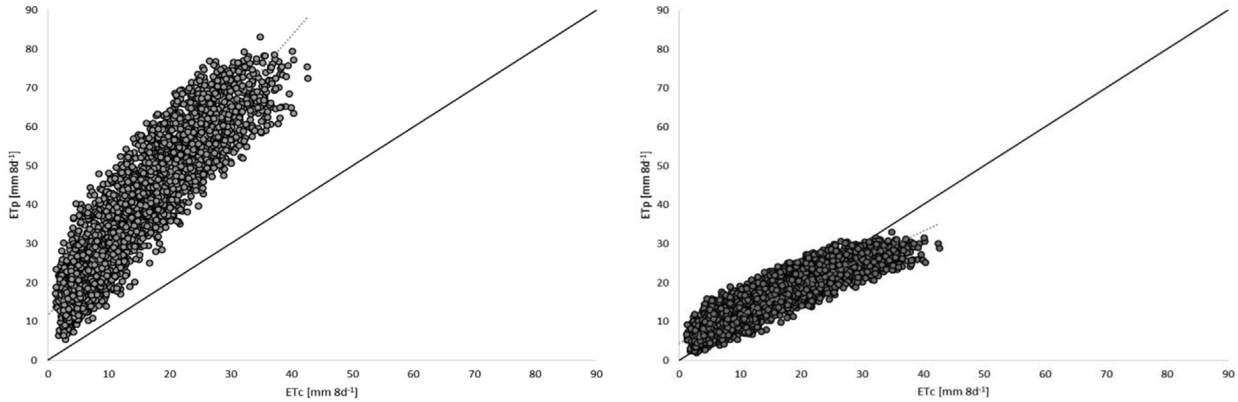

Fig. 6. Original $ETc_{(ORA)}$ vs $ETp_{(MOD16A2.006)}$ (left) Corrected $ETc_{(ORA)}$ vs $ETp_{(MOD16A2.006)}$ (right). Black line: 1:1 line.

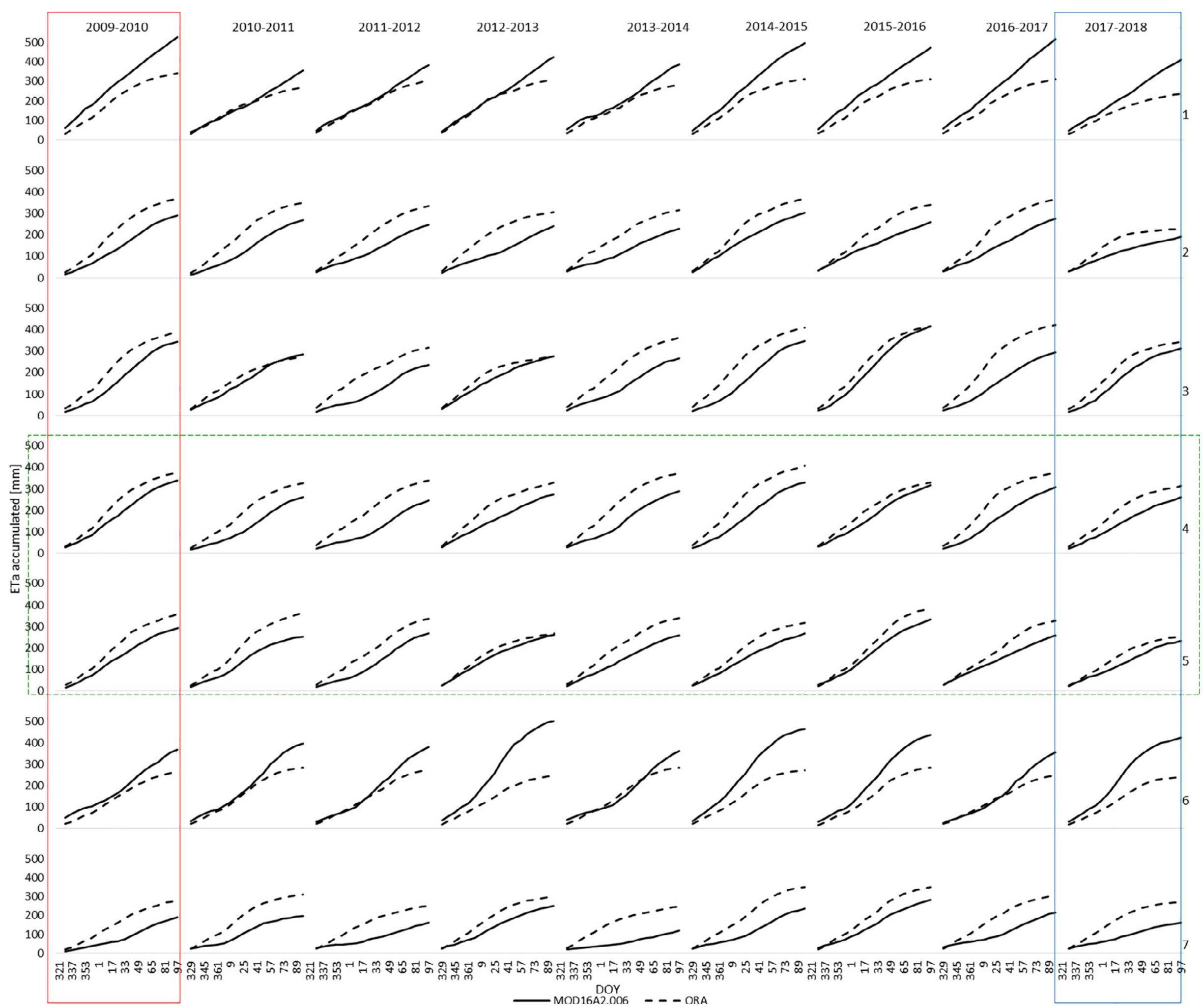

Fig. 7. Cumulative values of predicted $ETa_{(MOD16A2.006)}$-$ETa_{(ORA)}$. 1–7 (defined in Fig. 1).

higher proportion of surface vegetation cover, favored by a high soil water availability.

When we analysing the multi-temporal behavior (green box, dashed line), the General Pico (located at the western limit of the region, with semi-arid conditions) and Junín (located in the center of the APR, with sub-humid conditions) stations are considered. In these it can be seen that $ETa_{(MOD16A2.006)}$ product is underestimated every growth stages with smaller differences in the accumulated $ETa_{(MOD16A2.006)}$ values when the rainfall of the cycle was equal to or higher than the average (Fig. 8), without being able to assign a specific differentiation related with the climatic conditions of the zone.

With the objective of analyse the performance of $ETa_{(MOD16A2)}$ respect to nine growth stages, we determined the statistical metrics for all stations (Table 4). In particular, the average RMSE varies between 14 and 25 mm for all studied growing stages (from 2009–

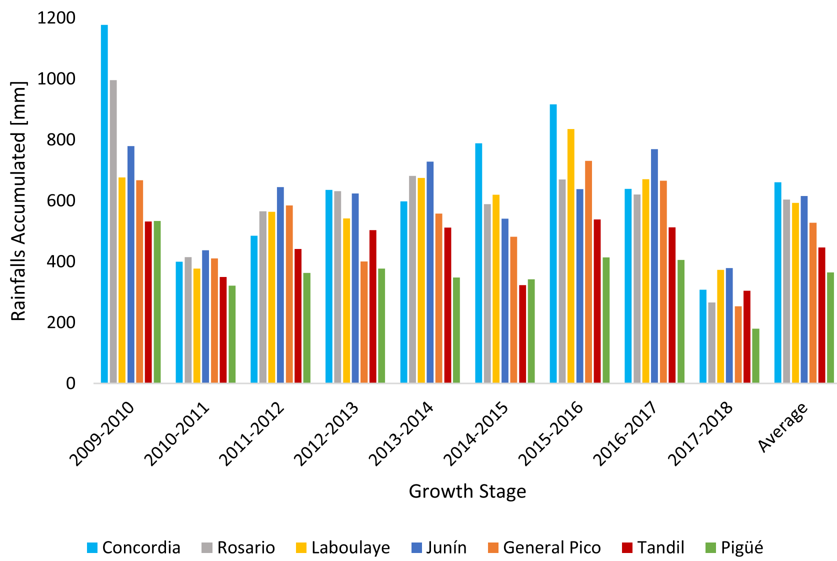

Fig. 8. Cumulative values of rainfalls in all sations in mm per growth stage.

Table 4
General statistics for all stations and growth stages.

Statistic [mm]	
RMSE	102.8
MBE	−6.75
MAE	89.01
a [adimensional]	−0.02
b	319.15

2010 to 2017–2018), being higher in the sub-humid humid zone, decreasing westward, in the semi-arid region.

When we evaluated the product in temporal resolution of $mm8d^{-1}$, we determined RMSE values (Table 5) result between 5.3 and 15.6 $mm8d^{-1}$ in subhumid-humid zone, while in semiarid zone the RMSE values are smaller, varying between 4 and 10.4 $mm8d^{-1}$.

About the performance $ETa_{(MOD16A2)}$ product in other latitudes (Table 1), we observed that in Mexican areas the errors associated to MOD16A2.006 product are 9.8, 6.2 y 3.2 $mm8d^{-1}$ for croplands, closed shrub and open shrub respectively (Aguilar et al., 2018). In Italy, they studied a heterogeneous and fragmented landscape with the presence of vineyards, olive trees, orchards and cereals, they observed an average RMSE of 7.1 $mm8d^{-1}$ (Peschechera et al., 2018). In APR the RMSE is greater than RMSE observed in other latitude, varying between 4 and 15.6 $mm8d^{-1}$ for soybean crop.

5. Conclusions

In this paper, we evaluated the performance of MOD16A2.006 actual and potential evapotranspiration product in Argentinian Pampas Region. MOD16A2.006 potential evapotranspiration product was compared with crop evapotranspiration, calculated with ground measurements using reference evapotranspiration (Penman-Monteith equation) from the *Oficina de Riesgo Agropecuario* and the crop coefficient data in seven stations in the Argentinian Pampas region from 2009 to 2018 period. Respect to potential evapotranspiration, we observed a systematic overestimation for MOD16A2.006 product of around 60%, with a RMSE (MAE) of 27.4 (24.6) $mm8d^{-1}$. We reduce this systematic error applying a linear adjustment equation. After calibration, statistical parameters improved significantly, resulting a RMSE (MAE) of 4.6 (3.5) $mm8d^{-1}$. The slope improved from 1.8 to 0.7 and intercept reduced from 11.6 to 4.4 $mm8d^{-1}$. These error values are expected from remote sensing measurement system. Applied this correction, we obtain appropriate potential evapotranspiration values for use in different studies (hydrology, agricultural, meteorology). It is concluded that, given existance of systematic error, it is required a correction to the MOD16A2.006 product in the Argentinian Pampas region before trusting the data directly provided.

We evaluated a MOD16A2.006 actual evapotranspiration product comparison with soil water balance data, at two temporal scales: in mm per growth stages (from 2009–2010 to 2017–2018) according to soybean crop, and in $mm8d^{-1}$. We concluded that the MOD16A2.006 actual evapotranspiration product has a

Table 5
RMSE values for each station and growth stages.

Growth Stages	RMSE [$mm8d^{-1}$]						
	Concordia	Rosario	Laboulaye	Junín	General Pico	Tandil	Pigüé
2009–2010	11.57	8.22	9.27	6.47	5.96	9.22	8.60
2010–2011	8.36	8.01	5.54	8.20	6.98	9.24	8.76
2011–2012	7.57	7.27	9.55	9.11	6.66	9.20	9.17
2012–2013	9.77	9.96	5.29	7.29	3.98	15.59	6.73
2013–2014	9.92	7.76	9.02	9.79	6.63	9.94	10.43
2014–2015	11.34	6.94	10.74	8.99	5.55	11.25	9.46
2015–2016	10.42	7.36	6.78	6.00	5.75	8.96	6.62
2016–2017	12.92	9.16	11.07	9.38	6.33	9.65	10.04
2017–2018	10.54	6.43	6.38	6.19	5.14	11.60	9.34

better performance in semi-arid areas than in humid-subhumid areas. In such regions, the satellite product underestimate in the most stations, while, in semiarid zones, the satellite values are close to ground measurements.

Declaration of Competing Interest

The authors declare that they have no known competing financial interests or personal relationships that could have appeared to influence the work reported in this paper.

Acknowledgments

The authors would like to thank the *Agencia Nacional de Promoción Científica y Tecnológica de Argentina* (PICT 2016-1486 project), FONARSEC FITS MAyCC N° 19/13 project and the *Comisión de Investigaciones Científicas de la Provincia de Buenos Aires* for their contributions. Also to the *Instituto de Hidrología de Llanuras*, the *Universidad Nacional del Centro de la provincia de Buenos Aires*, the Thermal Remote Sensing group of the University of Valencia through the project CGL2015-64268-R (MINECO/FEDER, UE), and the Sport, Culture and Education Council (JCCM, Spain), together with FEDER funds, throughout the ''ANIATEL'' project (SBPLY/17/180501/000357). Finally, we also thank the *Oficina de Riesgo Agropecuario* for providing ETa and ET_0 data and the University of Montana for providing the MOD16A2 data products.

References

Aguilar, A., Flores, H., Crespo, G., Marín, M., Campos, I., Calera, A., 2018. Performance Assessment of MOD16 in Evapotranspiration Evaluation in Northwestern Mexico. Water 10 (7), 901. https://doi.org/10.3390/w10070901.

Allen, R.G., Pereira, L.S., Howell, T.A., Jensen, M.E., 2011. Evapotranspiration information reporting: I. Factors governing measurement accuracy. Agric. Wat. Manag. 98 (6), 899–920. https://doi.org/10.1016/j.agwat.2010.12.015.

Allen, R.G., Pereira, L.S., Raes, D., Smith, M., 1998. Crop evapotranspiration-Guidelines for computing crop water requirements. Irrigation and Drainage Paper no.56. FAO, Rome, Italy.

Autovino, D., Minacapilli, M., Provenzano, G., 2016. Modelling bulk surface resistance by MODIS data and assessment of MOD16A2 evapotranspiration product in an irrigation district of Southern Italy. Elv. Agric. Wat. Manag. 167, 86–94. https://doi.org/10.1016/j.agwat.2016.01.006.

Carmona, F., Holzman, M., Rivas, R., Degano, M.F., Kruse, E., Bayala, M., 2018. Evaluation of two models using CERES data for reference evapotranspiration estimation. Rev. de Teledet. 51, 87–98. https://doi.org/10.4995/raet.2018.9259.

Chang, Y., Qin, D., Ding, Y., Zhao, Q., Zhang, S., 2018. A modified MOD16 algorithm to estimate evapotranspiration over alpine meadow on the Tibetan Plateau, China. J. Hydrol. 561, 16–30. https://doi.org/10.1016/j.jhydrol.2018.03.054.

Cleugh, H.A., Leuning, R., Mu, Q.Z., Running, S.W., 2007. Regional evaporation estimates from flux tower and MODIS satellite data. Rem. Sens. Env. 106 (3), 285–304. https://doi.org/10.1016/j.rse.2006.07.007.

Degano, M.F., Rivas, R.E., Carmona, F., Faramiñán, A., Olivera Rodríguez, P., 2018a. Calibración del producto de evapotranspiración potencial ''MOD16_A2'' para la Región Pampeana Argentina. Bol. Geol. y Min. España (approved for publication).

Degano, M.F., Rivas, R.E., Sánchez, J.M., Carmona, F., Niclòs, R., 2018b. Assessment of the Potential Evapotranspiration MODIS Product Using Ground Measurements in the Pampas. In Proc. IEEE, ARGENCON, San Miguel de Tucumán, Tucumán, Argentina, 2018, 1-5. Doi: 10.110 9/ARGENCON.2018.8646143

Didan, K., Barreto Munoz, A., Solano, R. and Huete., A., 2015. MODIS Vegetation Index User's Guide (MOD13 Series). Version3.

Hu, G., Jia, L., Menenti, M., 2015. Comparison of MOD16 and LSA-SAF MSG evapotranspiration products over Europe for 2011. Rem. Sens. Environ. 156, 510–526. https://doi.org/10.1016/j.rse.2014.10.017.

Kamble, B., Kilic, A., Hubbard, K., 2013. Estimating crop coefficients using remote sensing-based vegetation index. Remote Sensing 5 (4), 1588–1602.

Kottek, M., Grieser, J., Beck, C., Rudolf, B., Rubel, F., 2006. World map of the Köppen-Geiger climate classification updated. Meteorologische Zeitschrift 15 (3), 259–263. https://doi.org/10.1127/0941-2948/2006/0130.

Monteith, J.L., Unsworth, M.H., 1990. Principles of environmental physics. Edward Arnold, London.

Mu, Q.Z., Heinsch, F.A., Zhao, M.S., Running, S.W., 2007. Development of a global evapotranspiration algorithm based on MODIS and global meteorology data. Remote Sens. Env. 111 (4), 519–536. https://doi.org/10.1016/j.rse.2007.04.015.

Mu, Q.Z., Zhao, M.S., Running, S.W., 2011. Improvements to a MODIS global terrestrial evapotranspiration algorithm. Rem. Sens. Env. 115 (8), 1781–1800. https://doi.org/10.1016/j.rse.2011.02.019.

Mu, Q.Z., Zhao, M.S., Running, S.W., 2013. MODIS Global Terrestrial Evapotranspiration (ET) Product (NASA MOD16A2/A3). Algorithm Theoretical Basis Document. Collection 5. Numerical Terradynamic Simulation Group. College of Forestry and Conservation. University of Montana.

Nadzri, M.I., Hashim, M., 2014. Validation of MODIS Data for localized spatio-temporal evapotranspiration mapping. IOP Conf. Ser. Earth Environ. Sci. 18, (1). https://doi.org/10.1088/1755-315/18/1/012183 012183.

Pereyra, F., 2003. Ecorregiones de la Argentina. SEGEMAR. Buenos Aires, Argentina, pp. 189, ISSN 0328-2325.

Peschechera, G., Tarantino, E., Fratino, U., 2018. Crop water requirements estimation at irrigation district scale from remote sensing: a comparison between MODIS ET product and the analytical approach. in Proc. SPIE- RSCy2018, Paphos, Cyprus, 1-10. Doi: 10.1117/12.2326147

Ramoelo, A., Majozi, N., Mathieu, R., Jovanovic, N., Nickless, A., Dzikiti, S., 2014. Validation of Global Evapotranspiration Product (MOD16) using Flux Tower Data in the African Savanna, South Africa. Remote Sens. 6 (8), 7406–7423. https://doi.org/10.3390/rs6087406.

Reboratti, C., 2010. Un mar de soja: la nueva agricultura en Argentina y sus consecuencias. Rev. de Geograf. Norte Grande 45, 63–76. https://doi.org/10.4067/S0718-34022010000100005.

Ruhoff, A.L., Paz, A.R., Aragao, L.E., Mu, Q., Malhi, Y., Collischonn, W., Rocha, H.R., Running, S.W., 2013. Assesment of the MODIS global evapotranspiration using Eddy Covariance measurements and hydrological modelling in the Rio Grande basin. Hydrol. Sci. J. 58, 1–19. https://doi.org/10.1080/02626667.2013.837578.

Running, S.W., Mu, Q.Z., Zhao, M.S., 2017. MOD16A2 MODIS/Terra Net Evapotranspiration 8-Day L4 Global 500m SIN Grid V006 NASA EOSDIS Land Processes DAAC. Doi: 10.5067/MODIS/MOD16A2.006

World Meteorological Organization, 1994. Guía de prácticas hidrológicas. Adquisición de datos, análisis, predicción y otras aplicaciones. WMO-N°168, 5ªed, 273-303.

Zhang, K., Kimball, J.S., Running, S.W., 2016. A review of remote sensing based actual evapotranspiration estimation. WIREs Water 3, 834–853. https://doi.org/10.1002/wat2.1168.

Web References

Earth data (NASA), 2019. Earth data search. https://search.earthdata.nasa.gov/search?m=1.3579101562500002!-8.58251953125!7!1!0!0%2C2&q=MOD16A2%20V006 (accessed 23 September 2019) Web References.

Sustainable Development Goals: https://sustainabledevelopment.un.org. Last accessed: 2 April 2020.

http://files.ntsg.umt.edu/data/NTSG_Products/MOD16/. Last accessed 2 June 2018.